HEAT-INDUCED SHAPE MEMORY POLYURETHANE WITH INCLUSION OF PALM KERNEL OIL

Yap Saw Yin**,** Aula Aqila Yusrizal, Tuti Katrina Abdullah and Syazana Ahmad Zubir*

School of Materials and Mineral Resources Engineering, Engineering Campus, Universiti Sains Malaysia, 14300 Nibong Tebal, Pulau Pinang, Malaysia

*syazanazubir@usm.my

Abstract. The performance of the shape memory polyurethane (SMPU) elastomers depends on their chemical composition, crystallinity of soft segment and degree of phase separation. This paper reports the influence of varying the molar ratio of palm kernel oil polyol (PKO) on the tensile and shape memory behaviour of polyurethanes. The SMPUs were synthesized using polycaprolactone diol (PCL) and PKO as soft segments, 4,4 methylene-bis(cyclohexyl isocyanate) (HMDI), isophorone diisocyanate (IPDI) and 1,4-butanediol as the hard segments via two-step bulk polymerization method. The SMPUs were characterized using Fourier transform infrared spectroscopy, X-ray diffraction, differential scanning calorimetry, scanning electron microscopy, tensile and shape memory tests. The results showed that the increase of soft segment crystallinity has enhanced the microphase separation and shape fixity of SMPUs synthesized using the same hard segment content (40%). Also, PU with 20% of PKO molar ratio (PKO20HS40) demonstrated a higher modulus value, tensile strength, elongation at break (EB) and shape fixity. PU prepared using only IPDI as diisocyanate (100 IPDI) showed larger Young's modulus, EB and shape fixity than PU prepared using HMDI (100 HMDI). PU samples with combination of HMDI and IPDI as diisocyanate showed higher value of Young's modulus and tensile strength than PU prepared using HMDI and IPDI alone.

Keywords: polyurethane, palm kernel oil, soft segment crystallinity, shape memory behaviour

Article Info

Received 6th October 2021
Accepted 4th December 2021
Published 20th December 2021

ISSN: 1823-7010, eISSN: 2600-7444

Introduction

Shape memory materials have received increasing attention from researchers and scientists because they are able to memorize two shapes at different conditions. Shape memory polymers (SMPs) are less expensive, lightweight, easier to fabricate and sometimes able to demonstrate superior properties than shape memory alloy. Amongst the popular SMPs are polytetrahydrofuran, polyethylene terephthalate block copolymer, polylactide and polyurethane. SMPs have found application in various fields such as industrial, medical, textile, and electronics.

Shape memory polyurethane (SMPU) elastomers are common smart polymers that composed of polyol, isocyanate, and chain extender. When exposed to external stimuli, they can switch from temporarily deformed shape to a memorized permanent shape. The external stimuli can be in the form of heat, light, electricity, magnetism, and chemical stimuli [1]. The soft and hard segments are crucial to obtain shape memory properties in SMPU. The soft segments provide reversible phase transformation to obtain temporary shape while the hard segments retain the original shape of SMPU through chemical cross-linking by means of either physical interaction or chemical bonding [2]. Figure 1 shows the molecular mechanism of SMPU in exhibiting the shape memory effect [3].

SMPUs have such unique structural characteristic because of the inherent incompatibility between the hard and soft segments. This characteristic is directly associated to microphase separated morphology between hard and soft segments. The mechanical and physical properties can be enhanced by driving higher micro-phase separation between hard and soft segments and by improving the hydrogen bonding of inter-hard segments.

The characteristics of SMPU are affected by its main components which are polyol, diisocyanate, and chain extender. Toluene diisocyanate (TDI) and methylene diisocyanate (MDI) are the most employed diisocyanate for PU synthesis. However, the prolonged exposure to TDI and MDI vapours will cause irritation to eyes, skin, and respiratory tract. Moreover, both TDI and MDI show low thermal stability [4]. On the other hand, 4,4 methylene-bis(cyclohexyl isocyanate) (HMDI) and isophorone diisocyanate (IPDI) exhibit better light stability than aromatic isocyanate. They show better phase separation than the aromatic isocyanates as well as develop superior mechanical properties PU [5]. The combination of HMDI (aliphatic isocyanate) and IPDI (aromatic isocyanate) increase the restriction of chain mobility which will increase the rigidity and reduce the elongation of the HMDI and IPDI based PU [6].

Nowadays, most polyols utilised in the PU industry are petrochemical based. However, currently, the petrochemical based polyols are facing a rising in price, depleting at high rate and require high technology processing system. The best alternative to synthesize polyols is using biodegradable resources such as palmeric oil, vernonia oil, castor oil, and cardanol oil to replace the petrochemical-based polyol [7]. Palm kernel oil composes of triglycerides, a naturally occurring fats, which are water-insoluble substances. The palm kernel oil undergoes polycondensation and esterification to form monoester with hydroxyl groups, which is the palm kernel oil polyol (PKO) used in this work.

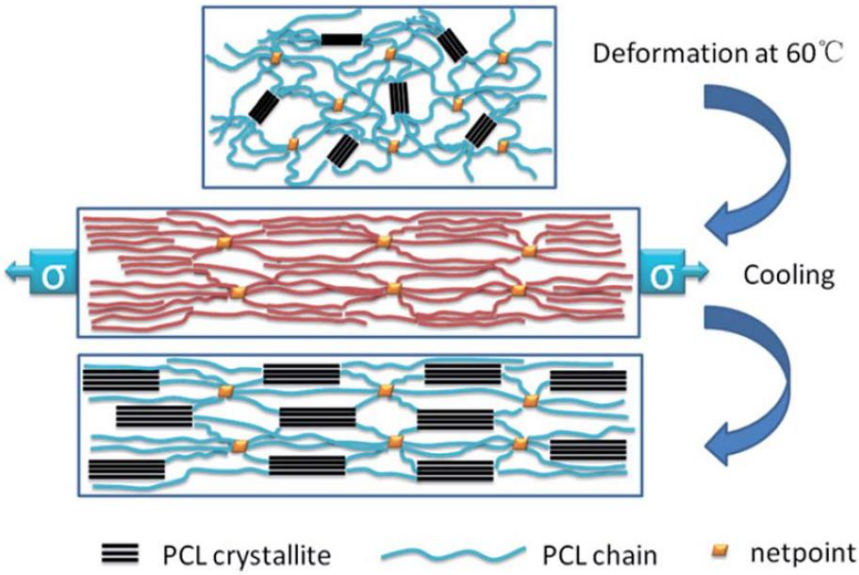

Figure 1. Shape memory mechanism of SMPU (reproduced with permission from RSC Publishing from reference [3])

In this study, PKO is used to replace certain portion of petrochemical based polyol. The aim of this research was to reduce the usage of petrochemical-based polyol in SMPU by substituting the palm kernel oil polyol as soft segment during SMPU synthesis. The usage of PKO-based feedstock can reduce environment impact by reducing the depletion of fossil fuel. Besides, the palm kernel oil polyol is believed to be able to improve the characteristics of SMPU. The influence of PKO molar ratio on the soft segment crystallinity, tensile and shape memory behaviour of SMPU were studied while the hard segment content (HSC) of polyurethane was fixed at 40%. Two-step bulk polymerization technique was employed to provide typical soft-hard-soft block sequence.

Materials and Methods

Materials. Polycaprolactone diol (PCL) with molecular weight 2000 g/mol was purchased from Sigma-Aldrich (Selangor, Malaysia) whereas palm kernel oil (PKO) with molecular weight 435 g/mol was supplied by Universiti Kebangsaan Malaysia. All of the polyols were vacuum dried in an oven at 80 °C overnight in order to eliminate moisture present. 4,4’ methylene-bis(cyclohexyl isocyanate) (HMDI), isophorone diisocyanate (IPDI), 1,4-butanediol (BD) and dibutyltin dilaurate were supplied by Sigma-Aldrich (Selangor, Malaysia). BD was pre-heated for 2 hours at 80 °C prior to use while HMDI and IPDI were used as received.

Synthesis of polyurethane prepolymer. PU was synthesised using two-step polymerization process. Using three neck flask dipped in an oil bath at a temperature of 80 °C, vacuum dried PCL, PEG, HMDI and IPDI were allowed to react under nitrogen atmosphere for 2.5 hours. PKO was added dropwise to the mixture and stirred for 2 hours. In the next step, BD and a few drops of DBTDL were added to the prepolymer in Haake internal mixer and mixed for 15 minutes at 90 °C. The rotor speed was set at 50 rpm. The PU samples were then hot pressed with preheating time 8 minutes and pressed for 3 minutes into 0.5 mm thick sheet using compression moulding at 160 °C and 1000 psi pressure.

The samples were coded as PKOXHS40 in which X refers to the molar ratio of PKO that was varied from 10 to 50%. For PU sample prepared with only HMDI (sample code 100HMDI) and IPDI (sample code 100IPDI) as diisocyanate, the samples were prepared using 20% PKO. The HSC of all PU samples was maintained at 40%.

Fourier Transform Infrared Spectroscopy (FTIR). FTIR spectrometer (Perkin Elmer Spectrum One FTIR Spectrometer) was used to analyse PU samples. Attenuated total reflectance (ATR) technique was used during the analysis of PU samples. Each sample was scanned 32 times with wavelength number recorded from 4000 cm^{-1} to 550 cm^{-1}[8].

Differential Scanning Calorimeter (DSC). DSC Mettler Toledo, Perkin Elmer was employed to determine the transition temperature (T_{trans}) of PU. The samples were heated from 30°C to 120°C at a rate of 10°C/min. This testing was carried out under nitrogen atmosphere flow with a heating rate of 10°C/ min. The percent crystallinity (X_c %) of the soft segments of SMPUs were calculated using the equation below:

$$\text{Percent crystallinity, } X_c\,\% = \Delta H_m / \Delta H^\circ_m \times 100\% \quad (1)$$

where ΔH°_m of 100% crystalline PCL = 136 Jg^{-1} [9]

X-ray Diffraction (XRD) Measurement. X-ray diffractometer (Bruker D8 Advance) was used to investigate the crystalline phase of PU. This device used Cu Kα (λ = 1.542 Å) as radiation source. The scattering angle (2θ) measurement was set from 10° to 40° with a scan rate of 1°/min.

Tensile Testing. Universal Testing Machine (UTM) model Instron 5982 was used to perform the tensile test. The PU sample was prepared in dumb-bell shape according to ASTM D638-type V. The testing was conducted with a load of 5 kN and crosshead speed of 50 mm/min. At least 5 specimens were tested to get average reading.

Shape Memory Testing. Rectangular sheet samples were used for shape memory test. The sheet was bent at a transition temperature, T_{trans} ±20°C to form a temporary ring-like shape. After that, the ring-shaped sample was placed in an ice-water bath for 10 minutes to cool rapidly to 3 °C. The deforming stress was removed and the resulting change in angle was measured as constraint removal angle, θ_{cr}. Then, the sample was reheated to temperature T_{trans} ±20 °C and the final angle, θ_f was measured. This method is in accordance with the method of Ratna et al. [10]. The shape fixity and shape recovery were calculated using equation (2) and (3).

$$\text{Shape fixity (\%)} = \theta_{cr}/90° \text{ x } 100 \quad (2)$$

$$\text{Shape recovery (\%)} = (90 - \theta_f)/\ 90° \text{ x } 100 \quad (3)$$

Scanning Electron Microscope (SEM). The tensile fractured surface of SMPU samples were observed using field emission scanning electron microscope, FESEM (Carl Zeiss SUPRA 35 VP FESEM model). The samples were coated with gold-palladium before loading to SEM chamber. The working distance was about 5 - 10 mm with magnification of 500 X.

Results and Discussion

FTIR Analysis. FTIR analysis was conducted in identifying the chemical bonds present in the samples. Figure 2 demonstrates the FTIR spectra of prepolymers and SMPUs. The characteristic vibrational absorption bands of prepolymers and PUs are almost at the same position.

The presence of peak at 3200-3600 cm^{-1} showed that OH groups was exhibited in all samples. The NH stretching peak observed at 3320-3360 cm^{-1} was overlapped with the OH peak. IR band at 1520-1640 cm^{-1} was assigned to the secondary –NH peaks [11]. The existence of –NH peaks indicates the complete formation of PU [12]. The CH_2 symmetrical stretching and CH_2 asymmetrical stretching were found at 2860-2870 cm^{-1} and 2930-2939 cm^{-1} respectively, whereas other modes of CH_2 vibrations were located at the bands of 1464, 1418, 1396, 1364 and 1294 cm^{-1} [13]. The band at 1000-1300 cm^{-1} could be assigned to (C-O-C) stretching vibrations [14].

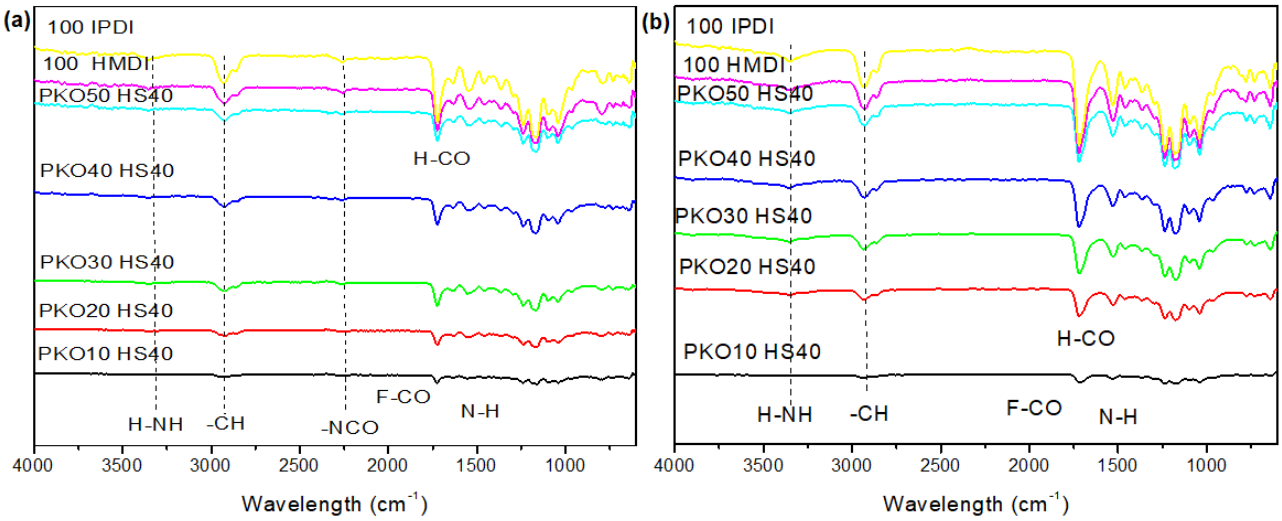

Figure 2. FTIR spectra of (a) prepolymers and (b) SMPUs

The C=O stretching vibrations were located at 1680-1760 cm^{-1} [15]. The C=O peak was split into two peaks. The stretching of free carbonyl groups was located at the sharp band centred near 1721-1730 cm^{-1}. The shoulder band centred at 1690-1701 was assigned to the stretching of hydrogen bonded carbonyl groups. The intensity of CO peak increased with the increase of PKO molar ratio, suggesting the existence of more CO groups with the addition of PKO (Figure 2b). The C-N stretching together with N-H in-plane bending were found at 1523-1537 cm^{-1}.

Bands at 2250-2270 cm^{-1} were assigned to the isocyanate (-NCO) groups. For PU samples, the absence of peaks in the range of 2250-2270 cm^{-1} indicates that the –OH groups of the polyols and chain extender have reacted with diisocyanate to form urethane linkages [16].

The phase separation can be analysed from the amount of hydrogen bonding of the urethane carbonyl (H-CO). From Figure 2(b), the carbonyl peak at the position of 1685 cm^{-1} broadened because of the formation of larger hard segment domains. At this position, free

carbonyl (F-CO) peak overlapped with the H-CO peak. A stronger H-CO peak indicates a higher degree of phase separation [17].

Soft segment crystallinity. Figure 3 and Table 1 show the thermal characteristics of SMPU based on DSC analysis. The endothermic peak observed at around 42-50 °C was related to the melting of soft segment PU (Figure 3). The melting point (T_m) increase as the PKO molar ratio was increased to 30% and then reduced with further increasing of the PKO content. On the other hand, samples prepared using one type of diisocyanate showed lower T_m as compared to the samples prepared using combined diisocyanate. The result indicates that combination of IPDI and HMDI has facilitated the crystallization of PU soft segment. Hence, a higher energy is required to melt more soft segment crystals.

Table 1. Thermal Characteristics of SMPUs

Sample	T_m(°C)	ΔH_m (Jg^{-1})	Crystallinity （%）
PKO10HS40	46.66	46.19	33.96
PKO20HS40	49.38	24.75	18.19
PKO30HS40	50.02	18.36	13.50
PKO40HS40	45.42	28.67	21.08
PKO50HS40	45.81	23.73	17.45
100HMDI	42.31	15.02	11.04
100IPDI	42.26	19.01	13.98

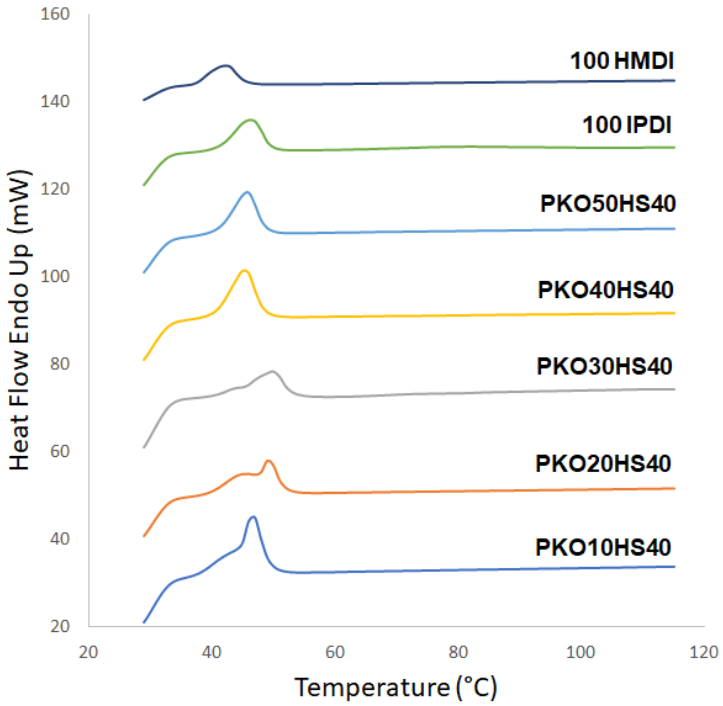

Figure 3. DSC thermogram of SMPUs

In general, the soft segment crystallinity was reduced with increasing molar ratio of PKO. It is as expected since PCL contributes to the formation of crystalline structure, hence as more PKO was used in the PU formulation, less PCL was added. The result suggests that the less phase separation was obtained as more PKO content was added since less

crystallization was observed. According to Liow et al. crystallization from both hard segments and soft segments could improve the phase separation [18].

The crystallinity of SMPUs can also be observed via XRD analysis. Figure 4 displays the XRD pattern of the SMPUs samples with significant diffraction peaks at about 2θ = 21°and 23° owing to (110) and (200) planes of PCL crystals [19] together with a broad peak centred at 20 °C indicating the presence of amorphous component in SMPU.

In general, the intensity of crystalline peaks was reduced with increasing molar ratio of SMPU. However, PKO40HS40 sample showed a higher intensity as compared to other samples. On the other hand, SMPU samples prepared using only HMDI and IPDI showed the lowest peak intensity. The same trend was also observed in DSC analysis. HMDI and IPDI are both aliphatic and linear. IPDI molecular structure possesses a higher stearic hindrance as compared to HMDI. The combination of both structures as diisocyanate in the preparation of SMPU might have promoted the formation of hard segment domains and enhanced the phase separation thus assisted the arrangement of ordered soft segment structures that contributed to a higher crystallinity. Ahmad et al. claimed that the formation of crystalline structure of SMPU was dependent on polyols, while the introduction of hard segments will change the crystallinity of copolymer which affected the phase compatibility [20]. Similar observation was found in this study.

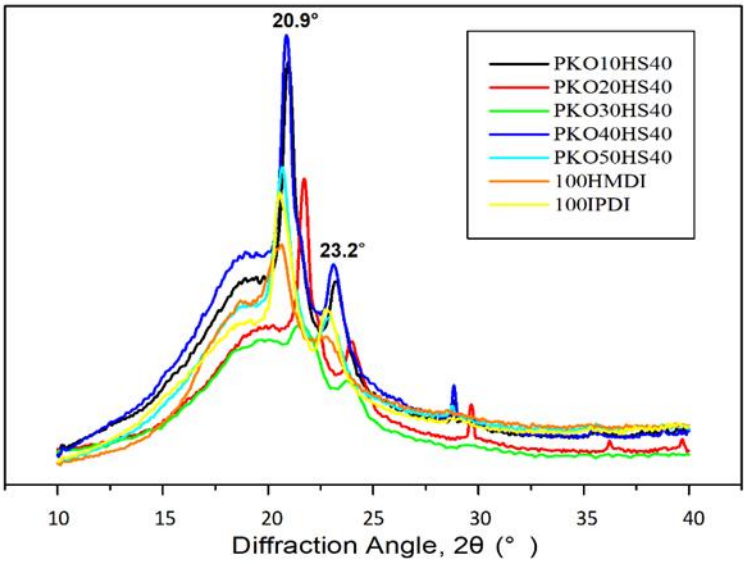

Figure 4. X-ray Diffractogram of SMPUs

Tensile properties and SEM morphology. Several factors affect the mechanical behaviour of the SMPU such as concentration and interconnectivity of hard segments, degree of crystallinity, degree of phase separation and presence of hydrogen bonding [21]. In general, the Young's modulus and tensile strength of SMPU were significantly improved as the crystallinity and phase separation were increased. Based on Table 2, as the molar ratio of PKO was increased, the tensile strength and Young's Modulus decreased. However, at 40% molar ratio of PKO, both values increased. This may be due to the high soft segment crystallinity present in the sample as observed in the DSC and XRD analysis.

It was noteworthy that the tensile properties for samples prepared using only HMDI and IPDI as diisocyanate were lower as compared to the SMPU samples prepared using the combination of both diisocyanate. This phenomenon was due to the combination of complex

structure of HMDI and IPDI as hard segments during preparation of SMPUs. The combination has restricted the chain mobility hence increased the rigidity and reduced the elongation of the PU [6]. The results obtained in this work have shown the advantage of combining different diisocyanate in the preparation of SMPU.

100IPDI showed higher Young's Modulus and crystallinity than 100HMDI at the same HSC due to the presence of rigid structure of cycloaliphatic IPDI molecules which provided polyurethanes a higher strength and rigidity. According to Javni et al. the stiffness of SMPU network was expected to increase by changing the structure of isocyanate in the following order: aliphatic < cycloaliphatic < aromatic [22]. This phenomenon is due to the rigid moiety of HMDI and IPDI coupled with dipole-dipole interaction and hydrogen bonding makes SMPU very difficult to stretch. In general, crystallinity causes the increase of brittleness and hardness of PU sample [23, 24]. Hence, elongation at break (EB) will increase with decreasing of crystallinity. However, in this study, the EB increased with increasing amount of PKO until PKO20HS40 where the highest value was achieved. Then, the EB of SMPUs decreased with further increase amount of PKO content. This is possibly because of enhanced molecular mobility induced by addition of PKO.

The PKO20HS40 showed the highest elongation at break which may be due to a higher miscibility between soft and hard domains. The increased miscibility enhanced the chain mobility and increased the elongation at break. On the other hand, other samples showed limited elongation. This phenomenon may be attributed to several factors. Firstly, PCL with moderate degree of crystallinity may acts as reinforcement filler and absorbed the deformation energy. Secondly, all the HMDI-BD segment of the polyurethanes were not crystalline [17].

Table 2. Tensile properties of SMPU

Samples	Modulus (MPa)	Tensile strength (MPa)	Elongation at break (%)
PKO10HS40	39.1 ± 4.3	4.0 ± 0.4	90.8 ± 21.3
PKO20HS40	27.9 ± 2.5	3.4 ± 0.2	327.1 ± 54.5
PKO30HS40	24.7 ± 3.1	2.7 ± 0.2	124.2 ± 44.1
PKO40HS40	34.2 ± 4.1	3.8 ± 0.2	126.8 ± 26.8
PKO50HS40	25.5 ± 2.0	2.9 ± 0.1	193.5 ± 41.5
100HMDI	16.5 ± 2.2	2.6 ± 0.3	124.6 ± 26.8
100IPDI	17.4 ± 1.0	1.7 ± 0.1	127.0 ± 37.1

Scanning electron microscope (SEM) was employed to analyse the morphology of tensile fractured surface of SMPUs (Figure 5). Distinct morphology was observed for samples with 20% PKO molar ratio; PKO20HS40 (HMDI and IPDI were used as diisocyanate), 100HMDI (only HMDI was used as diisocyanate) and 100IPDI (only IPDI was used as diisocyanate). 100IPDI showed smooth surface with fibrillar like structure whereas 100HMDI showed coarse tensile surface. On the other hand, PKO20HS40 showed a smoother matrix phase and pull-out due to tensile fracture as it possessed the highest elongation at break. The rest of the sample showed coarse structure due to the gradual fracture of specimens during tensile test. The soft-hard phases could be seen in PKO20HS40 and PKO30HS40 as the bumpy phase (red circles) associated to the hard phase meanwhile the soft segment is the smooth and continuous phase (red arrow) near the coarse structure as a result of gradual tensile fracture [25].

Shape memory properties. Shape fixity and shape recovery are the two important properties for describing SMPU's shape memory behaviour. The shape fixity defines the ability of switching segment (soft segment) to fix the mechanical deformation that is applied during deformation process [9] whereas the shape recovery describes the ability of hard segment to memorize the permanent shape. In general, the shape fixity of the synthesized SMPU decreased with the increase of PKO molar ratio (Table 3). The values of shape fixity were in accordance with the degree of soft segment crystallinity of SMPU. The higher the crystallinity, the higher the shape fixity such that the crystalline soft segment needed to fix the temporary shape [26]. This observation is further confirmed by the DSC analysis measurement where the PKO10HS40 showed the highest percent of crystallinity (34.0%).

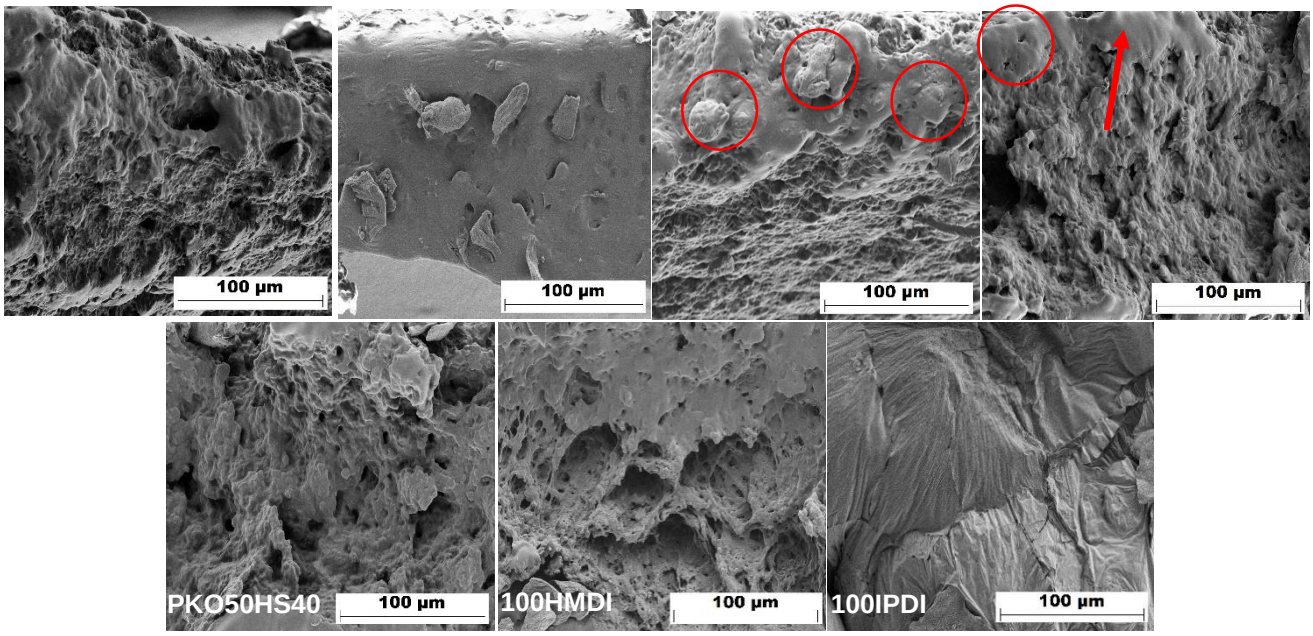

Figure 5. Morphology of fractured surface of SMPUs at 500x magnification

In summary, all samples showed good shape recovery of 100% indicating adequate amount of physical crosslinking present among the hard segment domains to fix the permanent shape (Table 3).

Table 3. Shape fixity and shape recovery of SMPUs

Samples Codes	Shape Fixity (%)	Shape Recovery (%)
PKO10HS4O	91.8	100
PKO20HS40	88.0	100
PKO30HS40	79.6	100
PKO40HS40	88.4	100
PKO50HS40	84.7	100
100HMDI	72.9	100
100IPDI	88.9	100

The hard segments from isocyanate and chain extenders should remain unperturbed to obtain effective shape recovery behaviour. Besides, the inter- or intra-polymer chain attractions as well as hydrogen bonding should be able to retain the physical cross-linking. Thus, the amount of hard segment domains (40%) in all samples were enough to produce sufficient physical cross-linking to recover its permanent shape.

Conclusion

SMPUs were successfully synthesized with different molar ratio of PKO via two-step bulk polymerization process. The results showed that with the increment of degree of phase separation and crystallinity of soft segment, the shape fixity was increased. The SMPUs produced exhibited better tensile properties with a higher Young's Modulus, tensile strength and shape fixity but a lower EB. PKO20HS40 with a Young's modulus of 27.9 ± 2.50 MPa, tensile strength of 3.39 ± 0.25 MPa, EB of 327.09 ± 54.49% and shape fixity of 88.0% was relatively the best among the polyurethanes with PKO molar ratio of 0.2. 100IPDI showed a higher Young's Modulus, EB and shape fixity than 100HMDI due to higher crystallinity and degree of phase separation. PU samples with combination of HMDI and IPDI as diisocyanate showed higher value of Young's Modulus and tensile strength than PU samples prepared using HMDI and IPDI as single diisocyanate.

Acknowledgements

The research was financially supported by the Ministry of Higher Education Malaysia for Fundamental Research Grant Scheme with Project Code: FRGS/1/2019/TK05/USM/03/2.

Author Contributions

All authors contributed toward data analysis, drafting and critically revising the paper and agree to be accountable for all aspects of the work.

Disclosure of Conflict of Interest

The authors have no disclosures to declare.

Compliance with Ethical Standards

The work is compliant with ethical standards.

References

[1] Xie, F., Huang, L., Leng, J. & Liu, Y. (2016). Thermoset shape memory polymers and their composites. *Journal of Intelligent Material Systems and Structures*, 27 2433-2455.

[2] Thakur, S. & Hu, J. (2017). *Aspects of Polyurethanes.* (IntechOpen) pp. 53-71

[3] Yang, P., Zhu, G., Shen, X., Yan, X. & Nie, J. (2016). Poly(ε-caprolactone)-based shape memory polymers crosslinked by polyhedral oligomeric silsesquioxane. *RCS Advances*, 93 (6) 90212-90219.

[4] Suryawanshi, Y., Sanap, P. & Wani, V. (2019). Advances in the synthesis of non-isocyanate polyurethanes. *Polymer Bulletin*, 76 3233-3246.

[5] Naheed, S., Shahid, M., Zahoor, R., Siddique, Z., Rasool, N., Haider, S. & Khan, S. (2021). Synthesis and Study of Morphology and Biocompatibility of Xanthan Gum/Titanium Dioxide-Based Polyurethane Elastomers. *Polymers*, 13 3416.

[6] Wu. H. M, Chen. J. F, Chen. S, Liu. S. F, Wang. M, Li. Fei & Wu. B (2014). Synthesis and properties of Cationic Waterborne Polyurethane Based on HMDI-IPDI. *Journal of University of South China (Science and Technology)*, 28 74-80.

[7] Alinejad, M., Henry, C., Nikafshar, S., Gondaliya, A., Bagheri, S., Chen, N., Singh, S.K., Hodge, D.B. & Nejad, M. (2019). Lignin-Based Polyurethanes: Opportunities for Bio-Based Foams, Elastomers, Coatings and Adhesives. *Polymers*, 11 1202.

[8] Mat Saad, N. & Ahmad Zubir, S. (2019). Palm kernel oil polyol- based polyurethane as shape
memory material: Effect of polyol molar ratio. *J. Phys. Sci*., 30(Supp. 2) 77–89.

[9] Kogikoski Jr, S., Liberato, M., M. Factori, I., Da Silva, E., Luis Pinto De Oliveira, C., Ando, R. & Alves, W. (2016). Polycaprolactone-Polyaniline Blend: Effects of the Addition of Cysteine on the Structural and Molecular Properties. *The Journal of Physical Chemistry C.*, 121 863-877.

[10] Ratna, D. & Karger-Kocsis, J. (2008). Recent advances in shape memory polymers and composites: a review. *Journal of Materials Science,* 43 254-269.

[11] Pereira, I.M., Gomide, V., Oréfice, R.L., Leite, Maria de F., Zonari, A.A.C. & Goes, Alfredo de M. (2010). Proliferation of Human Mesenchymal Stem Cells Derived from Adipose Tissue on Polyurethanes with Tunable Biodegradability. *Polimeros,* 20 (4) 280-286.

[12] Barikani, M., Valipour Ebrahimi, M. & Mohaghegh, S. (2007). Influence of Diisocyanate Structure on the Synthesis and Properties of Ionic Polyurethane Dispersions. *Polymer-Plastics Technology and Engineering*, 46 10-12.

[13] Ryszkowska, J. L., Auguścik, M., Sheikh, A. & Boccaccini, A. R. (2010). Biodegradable polyurethane composite scaffolds containing Bioglass® for bone tissue engineering. *Composites Science and Technology,* 70 1894-1908.

[14] Zhang, C., Hu, J., Chen, S. & Ji, F. (2010). Theoretical study of hydrogen bonding interactions on MDI-based polyurethane. *Journal of Molecular Modeling*, 16 1391-1399.

[15] Ti, Y., Wen, Q. & Chen, D. (2016). Characterization of the hydrogen bond in polyurethane/attapulgite nanocomposites. *Journal of Applied Polymer Science,* 133 (9) 43069.

[16] Ibrahim, S., Ahmad, A. & Mohamed, N.S. (2015). Synthesis and characterization of castor oil-based polyurethane for potential application as host in polymer electrolytes. *Bulletin of Materials Science*, 38 1155–1161.

[17] Hood, M. A., Wang, B., Sands, J. M., La Scala, J. J., Beyer, F. L. & Li, C. Y. (2010). Morphology control of segmented polyurethanes by crystallization of hard and soft segments. *Polymer*, 51 2191-2198.

[18] Liow, S. S., Lipik, V., Widjaja, L. K., Venkatraman, S. & Abadie, M. (2011). Enhancing mechanical properties of thermoplastic polyurethane elastomers with 1,3-trimethylene carbonate, epsilon-caprolactone and L-lactide copolymers via soft segment crystallization. *Express Polymer Letters*, 5(10) 897-910.

[19] Baptista, C., Azagury, A., Shin, H., Baker, C.M., Ly, E., Lee, R. & Mathiowitz, E. (2020). The effect of temperature and pressure on polycaprolactone morphology. Polymer, 19 122227.

[20] Ahmad, M., Luo, J., Xu, B., Purnawali, H., King, P. J., Chalker, P. R., Fu, Y., Huang, W. & Miraftab, M. (2011). Synthesis and Characterization of Polyurethane-Based Shape-Memory Polymers for Tailored Tg around Body Temperature for Medical Applications. *Macromolecular Chemistry and Physics*, 212 592-602.

[21] Lee D.W., Kim H.N. & Lee D.S. (2019). Introduction of Reversible Urethane Bonds Based on Vanillyl Alcohol for Efficient Self-Healing of Polyurethane Elastomers. *Molecules*, 24(12) 2201.

[22] Javni, I., Zhang, W. & Petrović, Z. S. (2003). Effect of different isocyanates on the properties of soy-based polyurethanes. *Journal of Applied Polymer Science*, 88 2912-2916.

[23] Gradinaru, R., Mihaela, M., Ciobanu, C., Filip, D., Macocinschi, D. & Vlad, S. (2011). Influence of diisocyanate structure on the properties of some polyetherurethanes based on renewable resources. *Journal of Optoelectronics and Advanced Materials*, 13(3) 286-292.

[24] Trinh, N.H., Jaafar, M., Viet, C.X. & Ahmad Zubir, S. (2020). Palm kernel oil polyol based shape memory polyurethane: effect of polycaprolactone and polyethylene glycol as soft segment. *Materials Research Express*, 7 (2) 025704.

[25] Das, S., Pandey, P., Mohanty, S., Nayak, S. K. (2015). Influence of NCO/OH and transesterified castor oil on the structure and properties of polyurethane: Synthesis and characterization. *Materials Express*, 5 377-389.

[26] Ahmad Zubir, S., Mat Saad, N., Harun, F.W. Ali, E.S. & Ahmad, S. (2018). Incorporation of palm oil polyol in shape memory polyurethane: Implication for development of cardiovascular stent. *Polymers for Advanced Technologies*, 29 (12) 2926-2935.